THE JOURNAL OF BIOLOGICAL CHEMISTRY
Vol. 279, No. 41, Issue of October 8, pp. 43000–43007, 2004
Printed in U.S.A.

A *Plasmodium falciparum* Dipeptidyl Aminopeptidase I Participates in Vacuolar Hemoglobin Degradation*

Received for publication, July 19, 2004, and in revised form, August 6, 2004
Published, JBC Papers in Press, August 10, 2004, DOI 10.1074/jbc.M408123200

Michael Klemba, Ilya Gluzman, and Daniel E. Goldberg‡

From the Departments of Medicine and Molecular Microbiology, Howard Hughes Medical Institute, Washington University School of Medicine, St. Louis, Missouri 63110

Intraerythrocytic growth of the human malaria parasite *Plasmodium falciparum* requires the catabolism of large amounts of host cell hemoglobin. Endoproteolytic digestion of hemoglobin to short oligopeptides occurs in an acidic organelle called the food vacuole. How amino acids are generated from these peptides is not well understood. To gain insight into this process, we have studied a plasmodial ortholog of the lysosomal exopeptidase cathepsin C. The plasmodial enzyme dipeptidyl aminopeptidase 1 (DPAP1) was enriched from parasite extract by two different approaches and was shown to possess hydrolytic activity against fluorogenic dipeptide substrates. To localize DPAP1 we created a transgenic parasite line expressing a chromosomally encoded DPAP1-green fluorescent protein fusion. Green fluorescent protein fluorescence was observed in the food vacuole of live transgenic parasites, and anti-DPAP1 antibody labeled the food vacuole in parasite cryosections. Together these data implicate DPAP1 in the generation of dipeptides from hemoglobin-derived oligopeptides. To assess the significance of DPAP1, we attempted to ablate DPAP1 activity from blood stage parasites by truncating the chromosomal DPAP1-coding sequence. The inability to disrupt the coding sequence indicates that DPAP1 is important for asexual proliferation. The proenzyme form of DPAP1 was found to accumulate in the parasitophorous vacuole of mature parasites. This observation suggests a trafficking route for DPAP1 through the parasitophorous vacuole to the food vacuole.

As the etiologic agent of severe malaria in humans, the Apicomplexan parasite *Plasmodium falciparum* is one of the leading causes of morbidity and mortality among infectious diseases. *P. falciparum* takes its greatest toll in sub-Saharan Africa, where at least 90% of the 1–2 million annual deaths due to falciparum malaria occur (1). The spread of parasites resistant to effective and affordable antimalarials such as chloroquine has led to a worsening of the situation. With a vaccine still many years away, the development of novel antimalarial chemotherapeutic agents that are efficacious against multidrug resistant parasites remains an urgent priority.

* This work was supported by National Institutes of Health Grant AI41718. The costs of publication of this article were defrayed in part by the payment of page charges. This article must therefore be hereby marked "*advertisement*" in accordance with 18 U.S.C. Section 1734 solely to indicate this fact.

‡ Recipient of a Burroughs Wellcome Fund Scholar Award in Molecular Parasitology. To whom correspondence should be addressed: Dept. of Molecular Microbiology, Howard Hughes Medical Institute, Washington University School of Medicine, 660 S. Euclid Ave., Box 8230, St. Louis, MO 63110. Tel.: 314-362-1514; Fax: 314-367-3214; E-mail: goldberg@borcim.wustl.edu.

Although *P. falciparum* has a complex life cycle that requires both mosquito and human hosts, the pathology caused by this parasite occurs while it reproduces asexually in human erythrocytes. During its intraerythrocytic development the parasite internalizes and degrades up to 75% of erythrocyte hemoglobin (2). Amino acids derived from hemoglobin catabolism are incorporated into plasmodial proteins (3), and parasites can rely on hemoglobin catabolism to supply sufficient quantities of all amino acids except those five that are rare in or absent from hemoglobin (4, 5). Based on these observations, a supply of amino acids for parasite protein synthesis has been considered the primary benefit of hemoglobin catabolism; however, recent studies suggest that this may not be the only benefit. A quantitative analysis of the incorporation of hemoglobin-derived amino acids into *P. falciparum* proteins has revealed that the parasite utilizes less than one-fifth of the amino acids made available through hemoglobin catabolism (6). This observation coupled with modeling of erythrocyte volume during intraerythrocytic growth has led to the suggestion that hemoglobin uptake and degradation may also be important in preventing hemolysis of *P. falciparum*-infected erythrocytes (7, 8).

In *P. falciparum*, hemoglobin is degraded in a single, acidic organelle known as the food vacuole or digestive vacuole. The initial stages of hemoglobin catabolism have been well characterized and involve a diverse set of endoproteinases. The initial proteolytic cleavage occurs at the hinge region of the α-globin chain and is mediated by the aspartic proteases plasmepsins I, II, and IV (9, 10). Further degradation of the globin chains is achieved through the action of plasmepsins I, II, and IV (10–12), histo-aspartic protease (11), and three cysteine proteases, falcipain-2, -2′, and -3 (13–15). The metalloprotease falcilysin converts short globin polypeptides into oligopeptides consisting of 5–10 amino acids (16). Inhibitors of both plasmepsins and falcipains block hemoglobin degradation and kill *P. falciparum* (5, 17). Interruption of hemoglobin catabolism is, therefore, an attractive strategy in the search for novel antimalarial chemotherapeutics.

The means by which oligopeptides are degraded to amino acids remain unclear. In a study addressing this question, Kolakovich *et al.* (50) asked whether amino acids can be generated from hemoglobin by food vacuole extract *in vitro*. The lack of detectable exopeptidase activity in this experiment suggested that hemoglobin catabolism may not occur to completion in the food vacuole. A model for hemoglobin degradation was proposed that envisioned export of hemoglobin-derived oligopeptides from the food vacuole to the cytoplasm for terminal degradation by neutral aminopeptidases. This model has been supported by the identification of cytosolic aminopeptidase activity in *P. falciparum* that can partially degrade hemoglobin peptides (18) and the description of a cytosolic zinc aminopeptidase with broad substrate specificity that is enriched at the cytosolic face of the food vacuole (19). However, direct evidence

for the transport of oligopeptides out of the food vacuole has not yet been reported.

To further our understanding of protein degradation in the food vacuole and to identify potential novel drug targets, we have mined the *P. falciparum* genome sequence data base for homologs of exopeptidases that function in acidic organelles. We identified a plasmodial homolog of mammalian type I dipeptidyl aminopeptidase (cathepsin C), a lysosomal exopeptidase that sequentially cleaves dipeptides from the N terminus of its oligopeptide substrate (20). Cathepsin C also plays a critical role in the activation of several serine proteases of immune effector cells (21–23). Given the role of cathepsin C in lysosomal protein degradation, we considered the possibility that the plasmodial enzyme might have a similar function in the food vacuole. To investigate this we undertook a detailed characterization of the *P. falciparum* dipeptidyl aminopeptidase, examining its enzymatic activity, its importance for asexual replication, and its location in the parasite.

EXPERIMENTAL PROCEDURES

Parasite Culture and Transfection—P. falciparum clones 3D7 and HB3 were cultured in human O^+ erythrocytes in RPMI 1640 supplemented with 27 mM sodium bicarbonate, 11 mM glucose, 0.37 mM hypoxanthine, 10 μg/ml gentamicin, and either 5 g/liter Albumax (Invitrogen; for routine growth) or 10% heat-inactivated human O^- serum (for transfection and cycling) as previously described (24). Cultures were synchronized by sorbitol treatment (25).

A dipeptidyl aminopeptidase type I (DPAP1)[1] truncation plasmid (pFA5KO) was made by PCR amplification of bases 928–1857 of the DPAP1 open reading frame from *P. falciparum* 3D7 genomic DNA with primers 5′-AGTCACTCGAGTAAGTTGTTGATAATGTAATAAATAAAGG (FA5KO1) and 5′-AGTCACTCGAGTTACCAACCTGTTATGTTATAGACAC and cloning the product into the XhoI site of pHC1 (26). The orientation of the insert was such that the 3′ end of the DPAP1 open reading frame was adjacent to the 5′ end of the HSP86 3′-untranslated region. The 3′ replacement construct (pFA5RE) was constructed in the same fashion by amplifying the 3′ 0.94 kilobases of the DPAP1 open reading frame with primers 5′-AGTCACTCGAGTAAGAGGTTACTAATCAATTATTATGTGG and 5′-AGTCACTCGAGTTAATTTCCTAATTCCTTTTGCATTTT. 3D7 ring-stage parasites were transfected with 50 μg of each plasmid using low voltage electroporation conditions (27), and resistant parasites were selected with 100 nM pyrimethamine. To enrich the population for parasites containing plasmid integrated into the DPAP1 locus, two rounds of drug cycling were carried out during which parasite cultures were grown for 21 days in the absence of drug to allow loss of the episome followed by reapplication of drug pressure (28).

To generate an in-frame fusion with GFPmut2 at the chromosomal DPAP1 locus, a 1.2-kilobase fragment of the 3′ end of the DPAP1 open reading frame (omitting the stop codon) was PCR amplified from *P. falciparum* 3D7 genomic DNA with primers FA5KO1 and 5′-GCACGCCTAGGATTTCCTAATTCCTTTTGCATTTTTTC and introduced into the XhoI/AvrII sites of pPM2GT (29) to yield pFA5GT. After electroporation of 3D7 rings with 100 μg of pFA5GT, parasites containing the plasmid were selected with 10 nM WR99210 and subjected to two drug cycles as described above. The transgenic parasites were then cloned by limiting dilution. Several clones were examined by fluorescence microscopy, and all had GFP distributions similar to that observed in the uncloned population. Clone F9 was selected for further analysis.

For Southern blotting, genomic DNA from parasite cultures was digested with either BsrG1/PvuI (pFA5KO and pFA5RE transfectants) or SpeI/NotI (pFA5GT transfectants), resolved on a 0.6% agarose gel, and transferred to a Hybond-N+ membrane (Amersham Biosciences). The membrane was blocked and probed with an alkaline phosphatase-labeled PCR product corresponding to bases 1169–1853 of the DPAP1 gene using the AlkPhos Direct kit (Amersham Biosciences).

Antibodies, Immunoblotting, and Immunoprecipitation—Recombinant DPAP1 lacking the first 27 amino acids was expressed as inclusion bodies in *Escherichia coli* and was used by the St. Louis University Hybridoma Development Service to generate monoclonal antibody 304.2.4.4 (abbreviated 244). This antibody recognizes an epitope in the DPAP1 exclusion domain (see Fig. 2*D*; data not shown). Polyclonal antibodies against DPAP1 were raised in rabbits (antiserum 1502; Cocalico Biologicals) against an eight-branch multiple antigenic peptide containing the sequence acetyl-TKKLDRKYLNNFDD (Research Genetics) and were affinity-purified against Sepharose-coupled peptide. Immunoblotting was carried out with monoclonal anti-DPAP1 antibody 244 (1:200; Figs. 2*C* and 5), affinity-purified rabbit anti-DPAP1 antibody1502 (1:500; Fig. 2*C*), affinity-purified rabbit anti-GFP antibody ab6556 (1:10,000, Abcam), rabbit anti-BiP (1:10,000 (30)), and mouse anti-P47/serine-rich antigen (SERA; 0.1 μg/ml (31)).

For immunoprecipitation, synchronized 3D7 or F9 trophozoites at 2% hematocrit and 10–15% parasitemia were labeled for 3 h in RPMI 1640 lacking cysteine and methionine (Sigma) supplemented as described under "Parasite Culture and Transfection" under "Experimental Procedures" and containing 90 μCi/ml [^{35}S]methionine and -cysteine (Expre^{35}S^{35}S, PerkinElmer Life Sciences). Labeled infected erythrocytes were washed three times with cold phosphate-buffered saline, resuspended in phosphate-buffered saline, and lysed by the addition of IP buffer (1× IP buffer is 50 mM Tris-HCl, pH 7.5, 150 mM NaCl, 6 mM EDTA, 1% Triton X-100, 0.5% deoxycholate, and the following protease inhibitors: 1 μM pepstatin, 10 μM *N*-acetyl-L-leucyl-L-leucyl-L-norleucinal, 1 μM *N*-(*trans*-epoxysuccinyl)-L-leucine-4-guanidinobutylamide, and 0.5 mM 4-(2-aminoethyl)-benzenesulfonyl fluoride). After removal of insoluble material, labeled proteins were immunoprecipitated at 4 °C with anti-DPAP1 antibody 244 (1:20) or Living Colors full-length A.v. polyclonal anti-GFP antibody (1:1000, BD Biosciences). Immune complexes were dissociated by boiling in reducing SDS-PAGE sample buffer, and proteins were analyzed by 12% SDS-PAGE and autoradiography.

DPAP1 Purification and Assay—DPAP1 was immunoprecipitated for 1 h at 4 °C from trophozoite lysate with monoclonal anti-DPAP1 antibody 244 and protein A-Sepharose beads (Amersham Biosciences) in 50 mM bis-tris-HCl, pH 7.0, 150 mM NaCl, 1 mM EDTA, 1 mM 4-(2-aminoethyl)-benzenesulfonyl fluoride, and 1 μM pepstatin (binding buffer). The beads were washed 3 times in binding buffer, once in wash buffer (10 mM bis-tris-HCl, pH 7.0, 150 mM NaCl) and were then added to assay mixtures containing 100 mM sodium acetate, pH 5.5, 50 mM NaCl, 1 mM dithiothreitol, 1 mM EDTA, and 100 μM β-naphthylamide substrate (Bachem). Assays were mixed continuously for 1 h at 37 °C, at which time the beads were removed by centrifugation. Supernatant fluorescence was measured on a PerkinElmer Life Sciences LS50B fluorimeter (335 nm excitation, 410 nm emission). Background fluorescence was determined from parallel samples lacking enzyme. In control experiments, no dipeptidase activity was detected if either the anti-DPAP1 hybridoma supernatant or the parasite extract was omitted or if hybridoma supernatant containing antibodies to the aspartic protease plasmepsin V (11) was used.

To purify DPAP1, ~5×10^9 saponin-treated clone HB3 trophozoites were suspended in 2 ml of lysis buffer (50 mM sodium malate, pH 5.2, 1 M $(NH_4)_2SO_4$, 1 mM EDTA, 1 μM pepstatin, and 2 μM leupeptin) and lysed by gentle sonication. Cell debris was removed by centrifuging at 100,000 × *g* for 1 h at 4 °C. The cleared supernatant was loaded onto a phenyl-Sepharose HP column (Amersham Biosciences) equilibrated with 50 mM sodium malate, pH 5.2, 1 M $(NH_4)_2SO_4$, and 1 mM EDTA, and DPAP1 activity was eluted with a linear gradient to 0 M $(NH_4)_2SO_4$. Active fractions were pooled, dialyzed against 50 mM bis-tris-HCl, pH 6.0, 1 mM EDTA, and loaded onto a Mono Q HR 5/5 column equilibrated with the same buffer. Protein was eluted with a linear gradient from 0 to 1 M NaCl. Active fractions were concentrated in a Centricon-10 microconcentrator (Amicon) and loaded onto a Superdex 75 column (Amersham Biosciences), equilibrated, and developed with 50 mM sodium acetate, pH 5.2, 100 mM Na_2SO_4, and 1 mM EDTA. Fractions containing DPAP1 activity were pooled and stored at 4 °C. All column steps were carried out at 4 °C. Protein purity was estimated to be 50% on SDS-polyacrylamide gels cross-linked with piperazine diacrylamide and stained with silver diamine according to the method of Hochstrasser as described (32). DPAP1 activity was assayed in 50 mM sodium MES, pH 6.0, 30 mM NaCl, 2 mM dithiothreitol, 1 mM EDTA, and 200 μM Pro-Arg-amidomethylcoumarin (Bachem). DPAP1 was activated for 10 min with 10 mM dithiothreitol before adding to substrate. Enzyme activity was monitored at ambient temperature as an increase in fluorescence (380 nm excitation, 460 nm emission). To generate a pH-activity profile, partially purified DPAP1 activity was measured with 100 μM Gly-Arg-amidomethylcoumarin (Bachem) in 50 mM citrate-

[1] The abbreviations used are: DPAP1, dipeptidyl aminopeptidase homolog 1; proDPAP1, DPAP1 proenzyme; PV, parasitophorous vacuole; SERA, serine-rich antigen; bis-tris, 2-[bis(2-hydroxyethyl)amino]-2-(hydroxymethyl)propane-1,3-diol; GFP, green fluorescent protein; MES, 4-morpholineethanesulfonic acid.

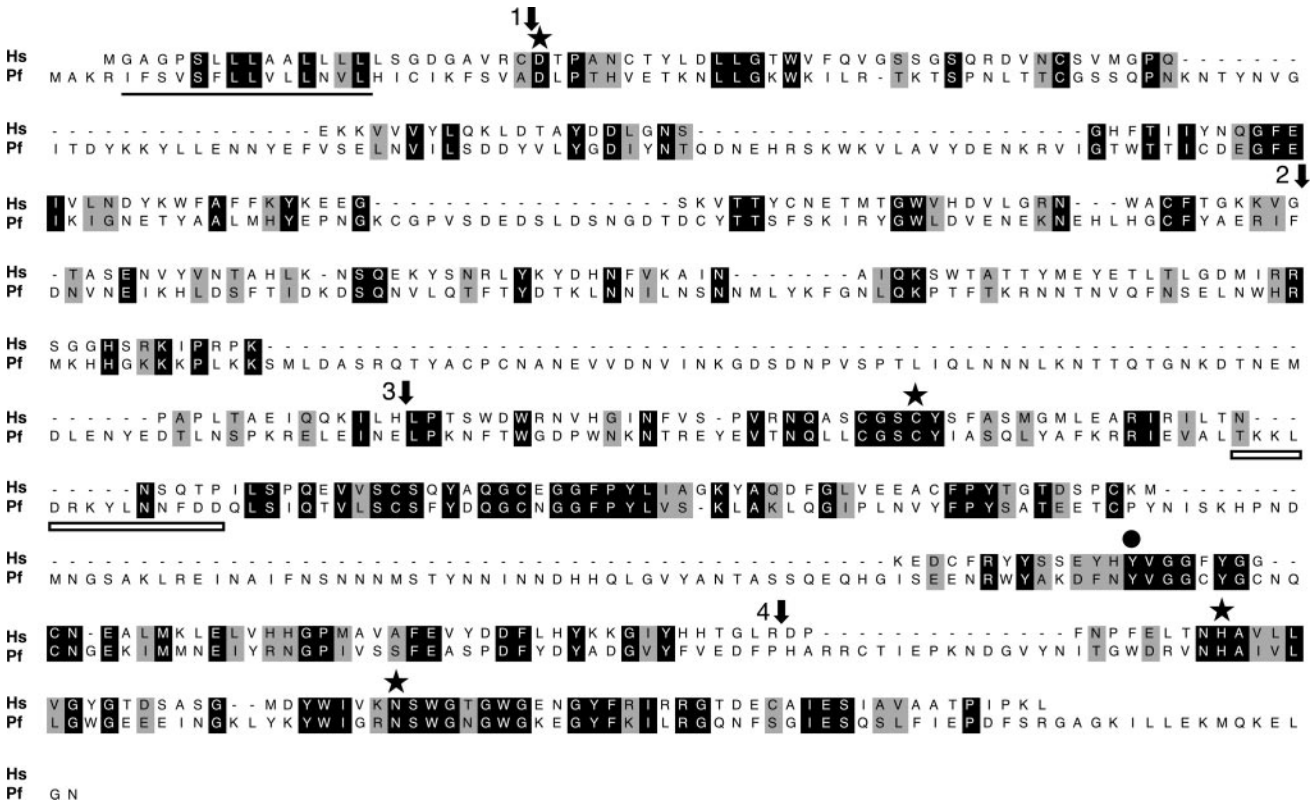

FIG. 1. **Alignment of human and plasmodial dipeptidyl aminopeptidase sequences.** Human cathepsin C (*Hs*; Swiss-Prot P53634) and DPAP1 (*Pf*) were aligned with ClustalW. Identical residues are *white* on a *black background*, and similar residues are *shaded gray*. Conserved active site residues are indicated with a *star*. A conserved tyrosine residue involved in chloride binding is denoted with a *black circle*. *Numbered arrows* indicate proteolytic cleavages that lead to mature human cathepsin C (44). *Arrows 1–2* delineate the exclusion domain, a cathepsin C-unique sequence that confers strict dipeptidyl aminopeptidase activity to this papain family cysteine protease; *arrows 2–3*, the excised prodomain; *arrows 3–4*, the catalytic region heavy chain; 4-end of sequence, the catalytic region light chain. The putative DPAP1 signal sequence is *underlined*, and the peptide sequence used to raise polyclonal antibodies is indicated with an *open box*.

phosphate buffers adjusted to pH values between 4.5 and 7.5 for 30 min at 37 °C.

Fluorescence and Immunoelectron Microscopy—Fluorescence and phase contrast images were collected with an Axioskop epifluorescence microscope equipped with a Plan-Neofluar Ph3 100x/1.3NA objective, an Axiocam CCD camera, and Axiovision 3.1 software (Carl Zeiss Microimaging). Parasites were mounted directly from culture and observed at ambient temperature. Parasite DNA was visualized by adding 5 μM Hoechst 33342 (Molecular Probes) immediately before mounting. Immunoelectron microscopy was performed on parasites fixed with 4% paraformaldehyde, 0.1% glutaraldehyde and immunogold-labeled with anti-GFP antibody 6556 (1:1000, Abcam) or anti-DPAP1 monoclonal antibody 244 (undiluted hybridoma supernatant) as previously described (29).

Parasite Fractionation—Erythrocytes infected with schizont stage parasites were enriched to 65–75% parasitemia on a 65% Percoll column (33). Saponin (Sigma) fractionation was carried out at a final concentration of 0.05% essentially as previously described (34). Fractionation with 3 μg/ml tetanolysin (35) was performed in a similar manner to that previously described for streptolysin O (36).

RESULTS

A Dipeptidyl Aminopeptidase Is Active in Blood Stage P. falciparum—We have identified three open reading frames encoding putative DPAP homologs (loci PF11_0174, PFL2290w, and PFD0230c) in a BLAST search of the *P. falciparum* genome sequence (37). A reverse transcription-PCR analysis of mRNA levels of the three homologs in intraerythrocytic parasites (data not shown) indicated that sequence PF11_0174 had a broad expression profile that included the stage during which the parasite was most actively degrading hemoglobin. In contrast, expression of the other two homologs was minimal in trophozoites and peaked in schizonts. From this analysis, PF11_0174 seemed to be the best candidate for a role in hemoglobin degradation and was, therefore, studied in greater detail. This sequence will be referred to here as *P. falciparum* DPAP homolog 1 or DPAP1.

The predicted amino acid sequence of DPAP1 shows significant homology to that of the human DPAP cathepsin C (Fig. 1). Identity/similarity over the exclusion domain, the prodomain, and the papain-like catalytic region is 26/40%, 16/32% and 38/54%, respectively (excluding gap positions). Over the entire sequence the two proteins share 30% identity and 45% similarity (excluding gap positions). Several residues known to be important for peptidase activity are conserved in DPAP1; they are Asp-28, which in cathepsin C is the N-terminal residue of the exclusion domain and blocks the substrate binding cleft beyond the P2 site (38, 39), and Cys-398, His-624, and Asn-648, which form the cysteine protease catalytic triad (40). A tyrosine residue that binds a chloride ion in the crystal structures of rat and human cathepsin C (38, 39) is also conserved (Tyr-549). The presence of a putative signal sequence at the N terminus of DPAP1 suggests that this protein transits the *P. falciparum* secretory system.

To determine whether DPAP1 exhibits dipeptidyl aminopeptidase activity, the protein was immunoprecipitated from soluble trophozoite extract with an anti-DPAP1 monoclonal antibody. The enzyme/antibody/protein A-Sepharose complex was then assayed against a panel of typical cathepsin C fluorogenic dipeptide substrates at pH 5.5, a value that is near the pH of the food vacuole lumen (41, 42). DPAP1 was active against six dipeptide substrates of diverse sequence, with highest activity against the dipeptide Pro-Arg (Fig. 2*A*). No activity was detected against substrates with blocked N termini, single amino acid substrates, a tripeptide substrate, or dipeptide substrates Lys-Ala and Gly-Pro (data not shown). Like cathepsin C (43),

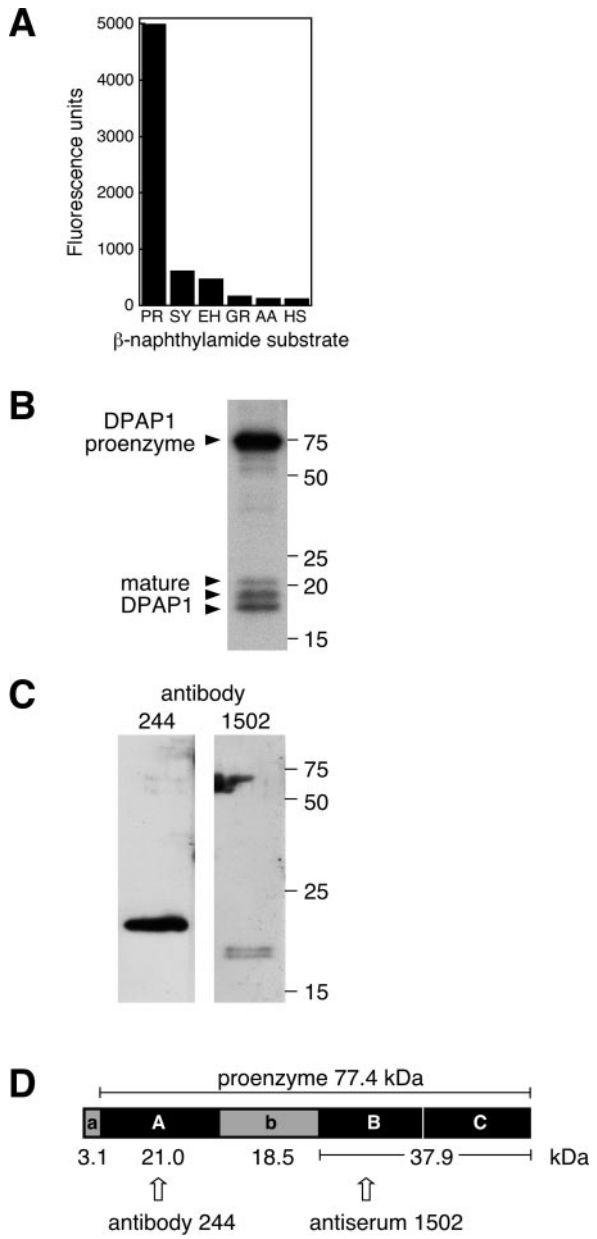

FIG. 2. **DPAP1 is an active dipeptidase that is proteolytically processed upon maturation.** *A*, activity of DPAP1 against a panel of β-naphthylamide dipeptide substrates. Dipeptide sequences are given *below* the *bars*. Fluorescence of enzymatically liberated β-naphthylamine was determined after a 1-h incubation at pH 5.5 with immunoprecipitated DPAP1. *B*, immunoprecipitation of pro- and mature DPAP1 from ^{35}S-labeled trophozoites. *C*, immunoblot analysis of partially purified DPAP1 using two DPAP1-specific antibodies. The detection of two closely spaced bands with antibody 1502 indicates that this polypeptide exhibits size heterogeneity in this preparation of partially purified enzyme. *D*, model for the processing of proDPAP1 to the mature enzyme based on the processing of human cathepsin C (44), the alignment in Fig. 1, and the polypeptide sizes in *B*. *Gray boxes* indicate sequences presumed to be absent from the mature enzyme. *a*, signal sequence. *b*, internal proregion. *Black boxes* indicate sequences composing mature DPAP1. *A*, the exclusion domain. *B* and *C*, the catalytic region, which is presumably cleaved (*vertical white line*) to generate two 18–19-kDa polypeptides. The polypeptides recognized by the two antibodies used in *C* are indicated. None of the polypeptide boundaries has been confirmed experimentally. In *B* and *C*, sizes of molecular markers are indicated in kDa.

DPAP1 cleaves unblocked dipeptide substrates, except for dipeptides having a basic residue in the first position or proline in the second position. To confirm that this activity was due to DPAP1 and not one of the other two DPAP homologs, soluble trophozoite extract was fractionated over consecutive hydrophobic interaction, anion exchange, and gel filtration columns. DPAP1 was observed to comigrate with dipeptidase activity (Fig. 2*C* and data not shown). In the pH range 4.5 to 7.5, DPAP1 activity was greatest at pH 5.5–6.0, with the activity at pH 7.5 only 5% of the value at pH 5.5 (data not shown). This result is consistent with a role for DPAP1 in the acidic lumen of the food vacuole.

The production of mature, active cathepsin C requires endoproteolytic processing of the proenzyme to remove the internal proregion (44). To determine whether DPAP1 is similarly processed, DPAP1 polypeptides were immunoprecipitated from ^{35}S-labeled trophozoites (Fig. 2*B*). A high molecular mass species was observed, the size of which is similar to that predicted for the proenzyme (proDPAP1) after signal peptide cleavage (77.4 kDa). In addition, three polypeptides with apparent molecular masses of 18–21 kDa were immunoprecipitated. By analogy with cathepsin C, these polypeptides were presumed to correspond to mature, active DPAP1 generated by excision of the prodomain and a single cleavage within the catalytic region (44). To confirm this, DPAP1 activity was partially purified from trophozoite extract by column chromatography and was subjected to immunoblotting with two DPAP1-specific antibodies (Fig. 2*C*). Only low molecular weight polypeptides and not the 77-kDa proenzyme were detected in the preparation of active DPAP1. Based on the known proteolytic processing sites in human cathepsin C (Fig. 1) and the sizes of the mature DPAP1 polypeptides (Fig. 2*B*), a model for the proteolytic activation of DPAP1 is proposed in Fig. 2*D*.

DPAP1 Is Important for Asexual Parasite Proliferation—To assess the importance of DPAP1 during the intraerythrocytic cycle, we attempted to disrupt the chromosomal copy of the DPAP1 gene by single-crossover recombination with a plasmid carrying a truncated segment of the coding sequence. The resulting protein would lack the last 81 residues, including the histidine residue of the catalytic dyad (Fig. 3*A*, *i*). As a control, integration of a 3′ replacement plasmid that carries the complete 3′ end of the coding sequence (and, therefore, does not truncate the protein) was attempted in parallel (Fig. 3*A*, *ii*). Parasites stably transfected with each plasmid were subjected to drug cycling to promote integration of the plasmids at the DPAP1 gene locus. A parasite population containing the integrated 3′ replacement plasmid was obtained after a single drug cycle (Fig. 3*B*). In contrast, no detectable integration of the truncation plasmid was observed after two drug cycles (Fig. 3*B*). The inability to force integration of the truncation plasmid suggests that inactivation of DPAP1 is lethal or highly deleterious to blood stage parasites.

DPAP1 Resides in the Food Vacuole—To localize DPAP1 in asexual blood stage parasites, we created a cloned line of parasites (designated F9) in which a sequence coding for a linker followed by GFP was integrated at the 3′ end of the coding region of the endogenous DPAP1 gene (Fig. 3, *A*, *iii*, and *C*). Immunoprecipitation of DPAP1 and GFP from F9 trophozoite extracts revealed that proDPAP1 was synthesized with the GFP tag, but that GFP was lost from mature DPAP1 (Fig. 3*D*). The loss of GFP was indicated by the close similarity of the sizes of mature DPAP1 polypeptides from F9 (Fig. 3*D*, anti-DPAP1 (*α-DPAP1*) *lane*) and wild-type 3D7 (Fig. 2*B*) parasites and by the appearance of a 27-kDa GFP species (Fig. 3*D*, anti-GFP (*α-GFP*) *lane*). These data also demonstrated that the GFP tag did not impede proper maturation of DPAP1. Because DPAP1 is an exopeptidase, cleavage of the linker between DPAP1 and GFP is probably mediated in *trans* by an endoprotease.

The distribution of GFP in live *P. falciparum*-infected erythrocytes was assessed by epifluorescence microscopy. The asex-

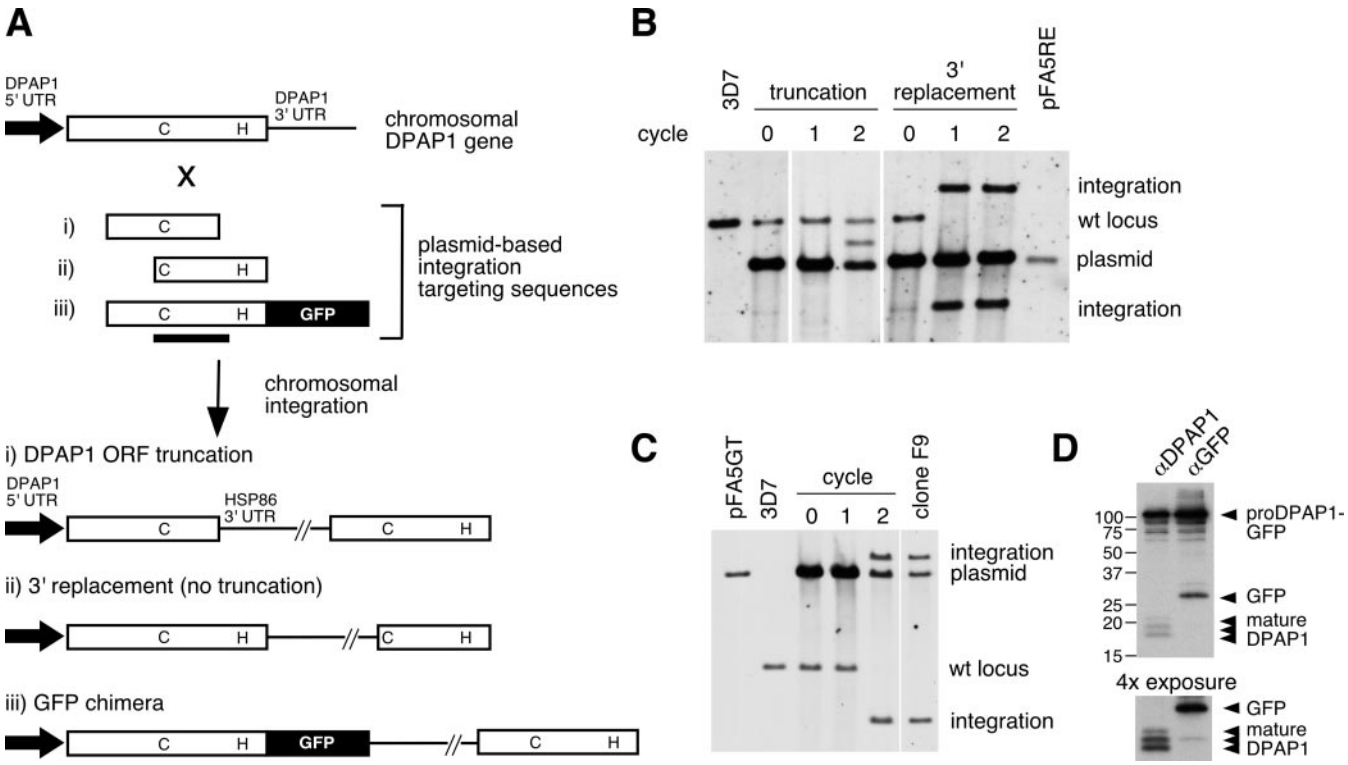

FIG. 3. **Attempted truncation of the endogenous DPAP1 coding sequence and creation of a chromosomally encoded DPAP1-GFP fusion.** *A*, schematic diagram of the strategy used for the modification of the DPAP1 gene locus through single-crossover recombination. Plasmids bearing the indicated targeting sequences were transfected into *P. falciparum* clone 3D7. The anticipated structure of the DPAP1 gene after integration of each plasmid is shown. For clarity, the plasmid backbone has been omitted. The positions of codons for the catalytic dyad Cys (C) and His (H) residues are indicated. The *black bar* marks the probe sequence used for Southern blots. *UTR*, untranslated region; *ORF*, open reading frame. *B*, Southern blot analysis of an attempt to truncate the DPAP1 coding sequence. Genomic DNA from untransfected (3D7) or transfected (truncation, 3′ replacement) cultures was probed. *Cycle 0* denotes a population of stable transfectants before cycling. The identities of the bands are given on the *right*. The new band that appears in the *cycle 2 lane* of the truncation experiment does not reflect recombination into the DPAP1 gene because the expected integration fragments do not appear; rather, it likely derives from episomal rearrangement or integration at another location in the genome. *wt*, wild type. *C*, Southern blot analysis of the creation of a transgenic parasite line containing a chromosomally encoded DPAP1-GFP chimera. Genomic DNA from untransfected (3D7) or transfected and drug-cycled parasites was probed. Genomic DNA from F9, a parasite line cloned after the second round of cycling, was also analyzed. The retention of a "plasmid" band in the clone F9 lane reflects the integration of tandem copies of the episome. *D*, immunoprecipitation from ^{35}S-labeled F9 trophozoite extract by anti-DPAP1 or anti-GFP antibody. Sizes of molecular markers are indicated in kDa on the *left*.

ual replicative cycle is typically divided into three morphologically distinct stages, the relatively quiescent ring stage (20–24 h in duration), the trophozoite stage (9–12 h), during which the parasite grows rapidly and copious amounts of hemoglobin are degraded, and the schizont stage (9–12 h), during which daughter merozoites develop and ultimately egress from the red cell in search of a new host. No GFP fluorescence was observed in ring-stage parasites (data not shown). In trophozoites and schizonts, accumulation of GFP in the food vacuole provided the first evidence that DPAP1 resides in this compartment (Fig. 4, *A–D*). To confirm that DPAP1 was transported to the food vacuole along with GFP, DPAP1 was localized by cryo-immunoelectron microscopy in F9 parasites. Immunogold label was abundant in the food vacuole, with occasional labeling outside of the food vacuole that may be associated with proDPAP1 in transit to the food vacuole (Fig. 4*E*). Food vacuole labeling was also observed in wild-type 3D7 parasites (data not shown). The relative abundance of both GFP (in the fluorescence images) and DPAP1 (in immunoelectron microscopy sections) in the food vacuole suggests that this compartment is the final destination for DPAP1 and supports the notion that DPAP1 contributes to hemoglobin catabolism.

Localization of DPAP1 to the Schizont Parasitophorous Vacuole and to Vesicles outside the Parasite—In schizonts, GFP fluorescence was observed in the parasitophorous vacuole (PV), the space between the closely apposed PV membrane and the parasite plasma membrane. The PV membrane forms around the parasite during invasion and remains intact until shortly before daughter merozoite egress (45, 46). In F9 schizonts undergoing nuclear division, PV fluorescence was evident as an outline around the periphery of the parasite (Fig. 4, *B* and *C*), whereas in mature segmented schizonts, the fluorescence could be seen around daughter merozoites (Fig. 4*D*). These schizont PV fluorescence patterns are similar to those reported previously in parasites expressing chimeric GFP proteins that target to the PV (47–49).

The presence of GFP in the PV raised the intriguing possibility that DPAP1 has a specific role in this compartment. To test whether proDPAP1 is processed to the catalytically active mature form in the PV, F9 schizonts were fractionated by treatment with tetanolysin, a protein that forms pores in the erythrocyte membrane, and with saponin, a detergent that permeabilizes both the erythrocyte and PV membranes (Fig. 5*A*). ProDPAP1-GFP was found in the saponin but not the tetanolysin supernatant, which indicates that this species is present in the PV but not in the erythrocyte cytosol (Fig. 5*B*). In contrast, neither GFP nor mature DPAP1 was detected in the saponin or tetanolysin supernatants. These species were found exclusively in the parasite pellets, a result consistent with residence within the food vacuole. These fractionation data indicate that proDPAP1 processing and GFP cleavage do not occur in the PV. To confirm that PV accumulation of DPAP1 is not an artifact of the GFP tag, wild-type 3D7 schizonts were fractionated with tetanolysin and saponin (Fig. 5*C*). Results

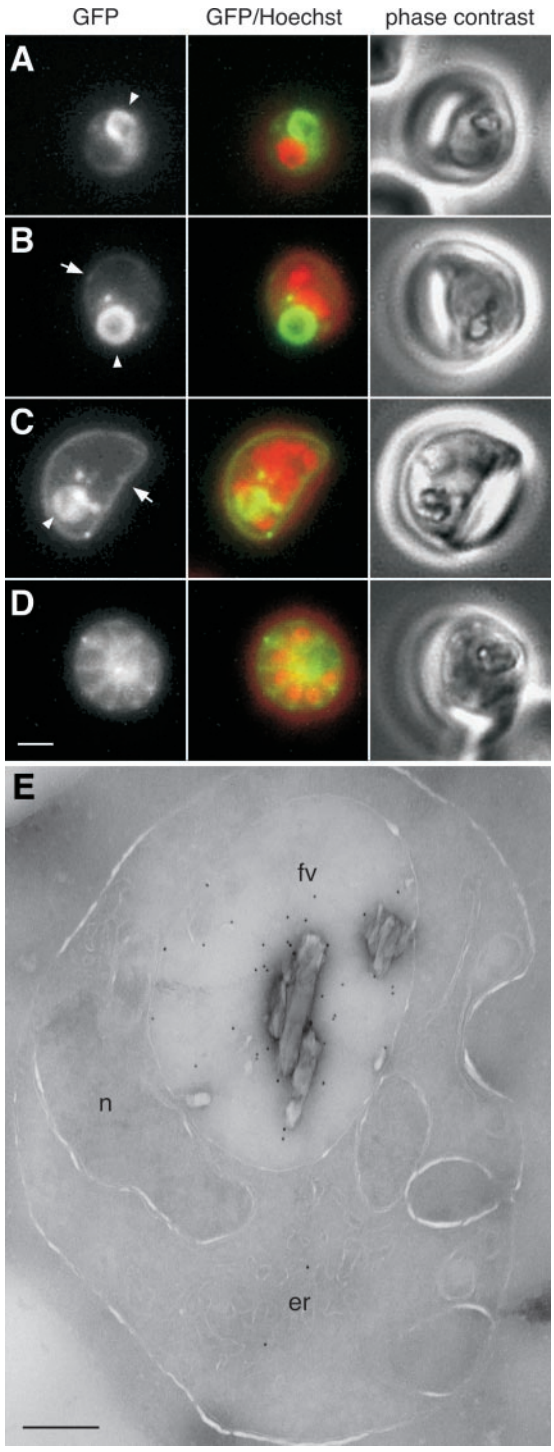

FIG. 4. **Localization of DPAP1 to the food vacuole and the parasitophorous vacuole.** *A–D*, fluorescence microscopy of live parasites expressing DPAP1-GFP. *A*, trophozoite. *B*, ~2N schizont. *C*, ~8N schizont. *D*, 8N segmented schizont. In the center column fluorescence from GFP is *green* and that from nuclear stain Hoechst 33342 is *red*. The food vacuole is indicated with *arrowheads* in the GFP *panels* of *A–C*, and the parasitophorous vacuole is indicated with *arrows* in *B* and *C*. Fluorescent spots in *B* and *C* may be vesicular structures involved in transport of DPAP1-GFP to the food vacuole. *Bar*, 2 μm. *E*, immunogold labeling of an F9 parasite with anti-DPAP1 antibody. *fv*, food vacuole; *er*, endoplasmic reticulum; *n*, nucleus. *Bar*, 400 nm.

were similar to those obtained with F9 parasites. In both experiments, the PV-resident 120-kDa SERA was used as an indicator of PV permeabilization, and the endoplasmic reticulum marker BiP was employed as a control for the integrity of the parasite.

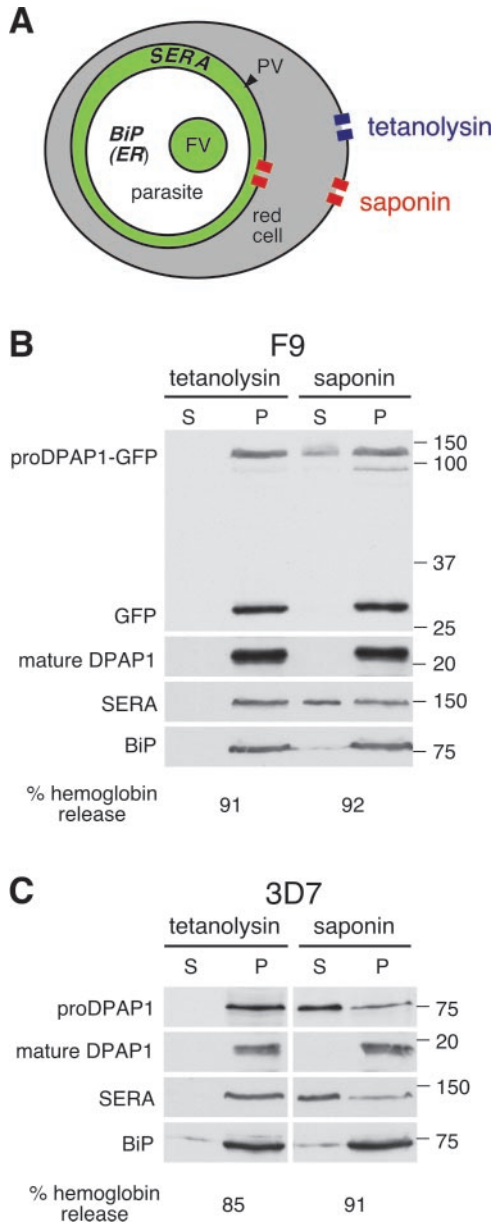

FIG. 5. **Fractionation of infected erythrocytes with tetanolysin and saponin.** *A*, schematic diagram of the effects of tetanolysin and saponin treatments. Tetanolysin (*blue pore*) permeabilizes the erythrocyte membrane, and saponin (*red pores*) permeabilizes both the erythrocyte and PV membranes. The food vacuole and PV are *shaded green* to signify the accumulation of GFP in these compartments, and the erythrocyte cytosol is *shaded gray*. Proteins used as compartment markers (BiP and SERA) are shown in *bold italics*. *B* and *C*, tetanolysin and saponin fractionation of F9 (*B*)- and wild-type 3D7 (*C*)-infected erythrocytes. Schizont cultures were treated with either 3 μg/ml tetanolysin or 0.05% saponin and separated into supernatant (*S*) and pellet (*P*) fractions. Proteins were detected by immunoblotting. Sizes of molecular mass markers are shown on the *right* in kDa.

In trophozoites and to a lesser degree in schizonts, bright GFP fluorescence was observed in mobile punctate spots. These spots became evident in very young trophozoites (Fig. 6*A*) and appeared to be outside the parasite yet were often very close to it with movement restricted to the outer parasite periphery. Occasionally, a fluorescent spot could be observed at a significant distance from the parasite. The average number of fluorescent spots per trophozoite was 3.6 ± 1.8 (n = 75). Treatment of infected erythrocytes with saponin did not result in loss of GFP from these structures (data not shown), which suggests that they are not contiguous with the parasitophorous vacuole/

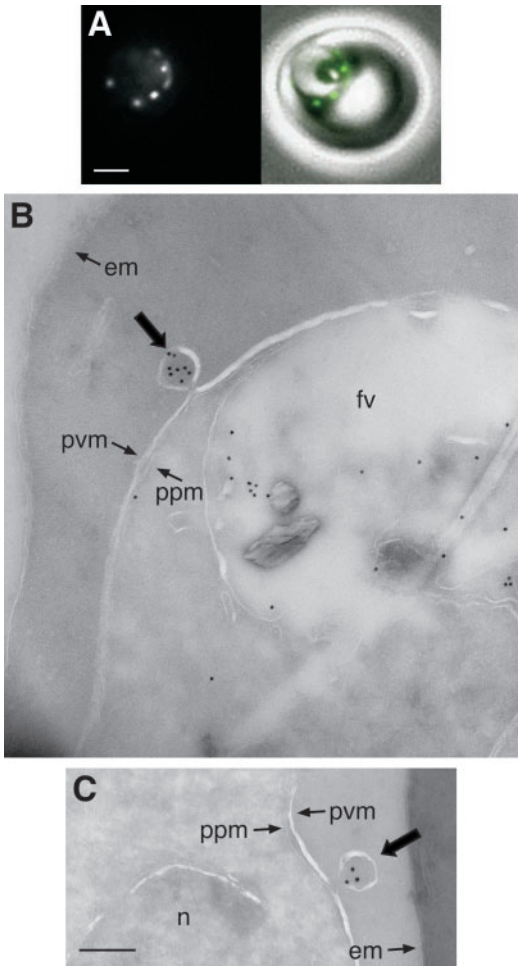

FIG. 6. **DPAP1-GFP accumulates in vesicles outside the parasite.** *A*, fluorescence image of a young F9 trophozoite showing GFP-containing foci (*left*) that in a fluorescence-phase contrast overlay (*right*) appear to lie outside the parasite. *Bar*, 2 μm. *B* and *C*, immunogold labeling of F9 parasites with either anti-GFP (*B*) or anti-DPAP1 antibody (*C*). Significant accumulations of gold label are observed in vesicles closely apposed to the parasitophorous vacuole membrane (*thick arrows*). *fv*, food vacuole; *ppm*, parasite plasma membrane; *pvm*, parasitophorous vacuole membrane; *em*, erythrocyte membrane; *n*, nucleus. *Bar*, 200 nm.

tubovesicular network, both of which are permeabilized by this detergent. Parasite cryosections labeled with anti-GFP or anti-DPAP1 antibody clearly show gold-filled vesicular structures with a diameter of 125–150 nm that are distinct from the parasitophorous vacuole (Fig. 6, *B* and *C*). These structures are unlikely to be involved in trafficking of DPAP1 outside of the parasite, as DPAP1 was not detected in either the erythrocyte cytosol (see above paragraph) or the culture media (data not shown).

DISCUSSION

Although the initial stages of hemoglobin degradation in the *P. falciparum* food vacuole have been intensely studied, the final steps in the conversion of globin peptides to amino acids have received scant attention. Oligopeptides of 5–10 amino were thought to be the end products of hemoglobin catabolism within the acidic food vacuole based largely on an *in vitro* analysis of hemoglobin degradation by food vacuole extract that failed to detect exopeptidase activity (50). Our results presented here strongly suggest that exopeptidase activity does indeed reside in the food vacuole. *P. falciparum* DPAP1, a cathepsin C ortholog, both possesses acidic dipeptidyl aminopeptidase activity and is located in the food vacuole at the

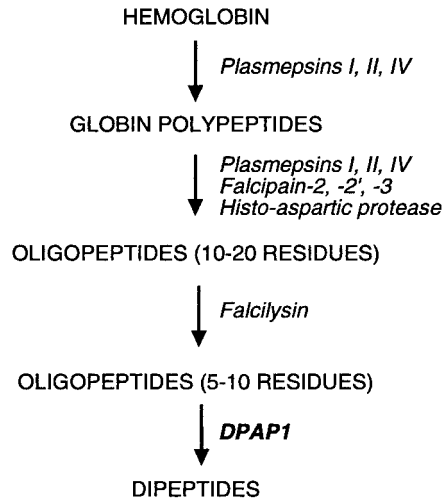

FIG. 7. **Peptidases contributing to the degradation of hemoglobin inside the *P. falciparum* food vacuole.** Endopeptidases are indicated in *italics*, and the sole known exopeptidase, DPAP1, is indicated in *bold italics*.

time of hemoglobin degradation. The probable role of DPAP1 is the release of dipeptides from the N termini of oligopeptides produced through the concerted action of food vacuole aspartyl-, cysteinyl- and metallo-endoproteases (Fig. 7). The failure to detect DPAP1 activity *in vitro* in food vacuole extract may derive from the lack of exogenously added reducing agent (50); a reducing environment is required to prevent oxidative inactivation of DPAP1 *in vitro* (data not shown).

How the dipeptides generated by DPAP1 are hydrolyzed to amino acids remains unclear. They may be actively transported out of the food vacuole in a similar fashion to that observed with lysosomes (51) for cleavage by cytosolic neutral aminopeptidases. Alternately, as-of-yet undiscovered acidic aminopeptidase activity may contribute to the hydrolysis of dipeptides within the food vacuole. Indeed, eight aminopeptidase homologs have been identified in the *P. falciparum* genome sequence (52), and only one these, a cytosolic M1 family zinc neutral aminopeptidase, has been characterized at the protein level (19, 53).

The inability to inactivate DPAP1 in blood stage parasites by truncation of the coding sequence provides evidence that its loss is lethal or highly deleterious to parasite proliferation. The importance of DPAP1 for intraerythrocytic growth makes this enzyme an attractive target for the development of novel antimalarial protease inhibitors that kill the parasite by blocking the later stages of hemoglobin degradation. This approach could complement current efforts to disrupt the early stages of hemoglobin degradation by inhibiting plasmepsins and falcipains (54). Although the two other cathepsin C homologs identified in the *P. falciparum* genome are expressed during the intraerythrocytic cycle (55, 56), they are apparently unable to compensate for the loss of DPAP1. If either of these homologs resides in the food vacuole, it may possess a complementary substrate specificity to that of DPAP1; alternately, these proteins may have functions completely unrelated to hemoglobin degradation. The presence of at least two cathepsin C homologs in the genome of the intestinal parasite *Cryptosporidium parvum* (57) provides a hint that these enzymes have roles to play in Apicomplexan biology outside of hemoglobin catabolism.

The presence of proDPAP1 but not mature DPAP1 in the PV of schizonts suggests a trafficking route for proDPAP1 to the food vacuole. In this model proDPAP1 would traffic to the PV via the parasite default secretory pathway (47–49). From there, proDPAP1 could be transported to the food vacuole in

double-membrane transport vesicles that bud from the cytostome, the site of hemoglobin endocytosis. The transport vesicles develop from an invagination of the PV and parasite plasma membranes (58); the space between these membranes is contiguous with the PV lumen and could be utilized to transport soluble proteins from the PV to the food vacuole. Transport of the membrane-anchored proplasmepsins I and II via cytostome-derived transport vesicles has been previously described (5, 29). The plausibility of this model for DPAP1 is supported by the observation that a fraction of the GFP in the PV of parasites expressing signal sequence-GFP fusions ends up in the food vacuole (47–49). Based on the steady-state amounts of GFP in the PV and food vacuole in these studies, this mode of transport appears relatively inefficient; therefore, DPAP1 may possess specific targeting signals directing it to the cytostome and, hence, to the food vacuole. The observed accumulation of proDPAP1 in the PV of schizonts but not trophozoites may simply derive from the reduction in cytostomal activity as the parasite matures. In the absence of a route out of the PV in schizonts, any newly synthesized DPAP1 would accumulate in this compartment.

In parasites expressing DPAP1-GFP, we observed mobile fluorescent spots outside the parasite. These spots are unlikely to be subdomains of the PV or tubovesicular network, as GFP was not released from them by saponin treatment. At ultrastructural resolution, these spots appeared to be vesicles in close apposition to the PV membrane. The only other structure to our knowledge that exhibits a punctate distribution in the erythrocyte cytosol is Maurer's clefts, which are implicated in trafficking of proteins to the erythrocyte membrane (59). The vesicles that we observe are not Maurer's clefts. At the ultrastructural level, Maurer's clefts appear as flattened, elongated cisternae near the erythrocyte membrane (60, 61) that may be part of a continuous membrane network that includes elements of the tubovesicular network (62). In contrast, the DPAP1-containing structures are round or irregular oval in shape and are in close proximity to the parasite. Moreover, Maurer's clefts are much more numerous than the three to four fluorescent spots that we typically observe in trophozoites (see for example Fig. 1 in Ref. 61). These intriguing structures will be the subject of further study.

Acknowledgments—We are very grateful to W. Beatty and L. LaRose for carrying out the immunoelectron microscopy, T. Horii for the anti-P47 (SERA) antibody, MR4 (ATCC, Manassas, VA) for providing us with anti-BiP antibody contributed by J. Adams, D. Jacobus (Jacobus Pharmaceuticals) for providing WR99210, and M. Drew and E. Istvan for critical reading of the manuscript.

REFERENCES

1. Greenwood, B., and Mutabingwa, T. (2002) *Nature* **415,** 670–672
2. Loria, P., Miller, S., Foley, M., and Tilley, L. (1999) *Biochem. J.* **339,** 363–370
3. Sherman, I. W., Ruble, J. A., and Tanigoshi, L. (1969) *Mil. Med.* **134,** 954–961
4. Divo, A. A., Geary, T. G., Davis, N. L., and Jensen, J. B. (1985) *J. Protozool.* **32,** 59–64
5. Francis, S. E., Gluzman, I. Y., Oksman, A., Knickerbocker, A., Mueller, R., Bryant, M. L., Sherman, D. R., Russell, D. G., and Goldberg, D. E. (1994) *EMBO J.* **13,** 306–317
6. Krugliak, M., Zhang, J., and Ginsburg, H. (2002) *Mol. Biochem. Parasitol.* **119,** 249–256
7. Lew, V. L., Tiffert, T., and Ginsburg, H. (2003) *Blood* **101,** 4189–4194
8. Lew, V. L., Macdonald, L., Ginsburg, H., Krugliak, M., and Tiffert, T. (2004) *Blood Cells Mol. Dis.* **32,** 353–359
9. Goldberg, D. E., Slater, A. F., Beavis, R., Chait, B., Cerami, A., and Henderson, G. B. (1991) *J. Exp. Med.* **173,** 961–969
10. Gluzman, I. Y., Francis, S. E., Oksman, A., Smith, C. E., Duffin, K. L., and Goldberg, D. E. (1994) *J. Clin. Investig.* **93,** 1602–1608
11. Banerjee, R., Liu, J., Beatty, W., Pelosof, L., Klemba, M., and Goldberg, D. E. (2002) *Proc. Natl. Acad. Sci. U. S. A.* **99,** 990–995
12. Wyatt, D. M., and Berry, C. (2002) *FEBS Lett.* **513,** 159–162
13. Shenai, B. R., Sijwali, P. S., Singh, A., and Rosenthal, P. J. (2000) *J. Biol. Chem.* **275,** 29000–29010
14. Sijwali, P. S., and Rosenthal, P. J. (2004) *Proc. Natl. Acad. Sci. U. S. A.* **101,** 4384–4389
15. Sijwali, P. S., Shenai, B. R., Gut, J., Singh, A., and Rosenthal, P. J. (2001) *Biochem. J.* **360,** 481–489
16. Eggleson, K. K., Duffin, K. L., and Goldberg, D. E. (1999) *J. Biol. Chem.* **274,** 32411–32417
17. Rosenthal, P. J. (1995) *Exp. Parasitol.* **80,** 272–281
18. Gavigan, C. S., Dalton, J. P., and Bell, A. (2001) *Mol. Biochem. Parasitol.* **117,** 37–48
19. Allary, M., Schrevel, J., and Florent, I. (2002) *Parasitology* **125,** 1–10
20. Kirschke, H., and Barrett, A. J. (1987) in *Lysosomes: Their Role in Protein Breakdown* (Glaumann, H., and Ballard, J., eds) pp. 192–238, Academic Press, Inc., London
21. Adkison, A. M., Raptis, S. Z., Kelley, D. G., and Pham, C. T. (2002) *J. Clin. Investig.* **109,** 363–371
22. Pham, C. T., and Ley, T. J. (1999) *Proc. Natl. Acad. Sci. U. S. A.* **96,** 8627–8632
23. Wolters, P. J., Pham, C. T., Muilenburg, D. J., Ley, T. J., and Caughey, G. H. (2001) *J. Biol. Chem.* **276,** 18551–18556
24. Trager, W., and Jensen, J. B. (1976) *Science* **193,** 673–675
25. Lambros, C., and Vanderberg, J. P. (1979) *J. Parasitol.* **65,** 418–420
26. Crabb, B. S., Triglia, T., Waterkeyn, J. G., and Cowman, A. F. (1997) *Mol. Biochem. Parasitol.* **90,** 131–144
27. Fidock, D. A., and Wellems, T. E. (1997) *Proc. Natl. Acad. Sci. U. S. A.* **94,** 10931–10936
28. Wu, Y., Kirkman, L. A., and Wellems, T. E. (1996) *Proc. Natl. Acad. Sci. U. S. A.* **93,** 1130–1134
29. Klemba, M., Beatty, W., Gluzman, I., and Goldberg, D. E. (2004) *J. Cell Biol.* **164,** 47–56
30. Kumar, N., Koski, G., Harada, M., Aikawa, M., and Zheng, H. (1991) *Mol. Biochem. Parasitol.* **48,** 47–58
31. Li, J., Mitamura, T., Fox, B. A., Bzik, D. J., and Horii, T. (2002) *Parasitol. Int.* **51,** 343–352
32. Rabilloud, T. (1992) *Electrophoresis* **13,** 429–439
33. Dluzewski, A. R., Ling, I. T., Rangachari, K., Bates, P. A., and Wilson, R. J. (1984) *Trans. R. Soc. Trop. Med. Hyg.* **78,** 622–624
34. Benting, J., Mattei, D., and Lingelbach, K. (1994) *Biochem. J.* **300,** 821–826
35. Lopez-Estrano, C., Bhattacharjee, S., Harrison, T., and Haldar, K. (2003) *Proc. Natl. Acad. Sci. U. S. A.* **100,** 12402–12407
36. Ansorge, I., Benting, J., Bhakdi, S., and Lingelbach, K. (1996) *Biochem. J.* **315,** 307–314
37. Gardner, M. J., Hall, N., Fung, E., White, O., Berriman, M., Hyman, R. W., Carlton, J. M., Pain, A., Nelson, K. E., Bowman, S., Paulsen, I. T., James, K., Eisen, J. A., Rutherford, K., Salzberg, S. L., Craig, A., Kyes, S., Chan, M. S., Nene, V., Shallom, S. J., Suh, B., Peterson, J., Angiuoli, S., Pertea, M., Allen, J., Selengut, J., Haft, D., Mather, M. W., Vaidya, A. B., Martin, D. M., Fairlamb, A. H., Fraunholz, M. J., Roos, D. S., Ralph, S. A., McFadden, G. I., Cummings, L. M., Subramanian, G. M., Mungall, C., Venter, J. C., Carucci, D. J., Hoffman, S. L., Newbold, C., Davis, R. W., Fraser, C. M., and Barrell, B. (2002) *Nature* **419,** 498–511
38. Olsen, J. G., Kadziola, A., Lauritzen, C., Pedersen, J., Larsen, S., and Dahl, S. W. (2001) *FEBS Lett.* **506,** 201–206
39. Turk, D., Janjic, V., Stern, I., Podobnik, M., Lamba, D., Dahl, S. W., Lauritzen, C., Pedersen, J., Turk, V., and Turk, B. (2001) *EMBO J.* **20,** 6570–6582
40. Storer, A. C., and Menard, R. (1994) *Methods Enzymol.* **244,** 486–500
41. Bennett, T. N., Kosar, A. D., Ursos, L. M., Dzekunov, S., Singh Sidhu, A. B., Fidock, D. A., and Roepe, P. D. (2004) *Mol. Biochem. Parasitol.* **133,** 99–114
42. Krogstad, D. J., Schlesinger, P. H., and Gluzman, I. Y. (1985) *J. Cell Biol.* **101,** 2302–2309
43. Callahan, P. X., McDonald, J. K., and Ellis, S. (1972) *Fed. Proc.* **31,** 1105–1113
44. Cigic, B., Krizaj, I., Kralj, B., Turk, V., and Pain, R. H. (1998) *Biochim. Biophys. Acta* **1382,** 143–150
45. Wickham, M. E., Culvenor, J. G., and Cowman, A. F. (2003) *J. Biol. Chem.* **278,** 37658–37663
46. Salmon, B. L., Oksman, A., and Goldberg, D. E. (2001) *Proc. Natl. Acad. Sci. U. S. A.* **98,** 271–276
47. Wickham, M. E., Rug, M., Ralph, S. A., Klonis, N., McFadden, G. I., Tilley, L., and Cowman, A. F. (2001) *EMBO J.* **20,** 5636–5649
48. Waller, R. F., Reed, M. B., Cowman, A. F., and McFadden, G. I. (2000) *EMBO J.* **19,** 1794–1802
49. Adisa, A., Rug, M., Klonis, N., Foley, M., Cowman, A. F., and Tilley, L. (2003) *J. Biol. Chem.* **278,** 6532–6542
50. Kolakovich, K. A., Gluzman, I. Y., Duffin, K. L., and Goldberg, D. E. (1997) *Mol. Biochem. Parasitol.* **87,** 123–135
51. Thamotharan, M., Lombardo, Y. B., Bawani, S. Z., and Adibi, S. A. (1997) *J. Biol. Chem.* **272,** 11786–11790
52. Wu, Y., Wang, X., Liu, X., and Wang, Y. (2003) *Genome Res.* **13,** 601–616
53. Florent, I., Derhy, Z., Allary, M., Monsigny, M., Mayer, R., and Schrevel, J. (1998) *Mol. Biochem. Parasitol.* **97,** 149–160
54. Rosenthal, P. J. (1998) *Emerg. Infect. Dis.* **4,** 49–57
55. Bozdech, Z., Llinas, M., Pulliam, B. L., Wong, E. D., Zhu, J., and DeRisi, J. L. (2003) *PLoS Biol.* **1,** 85–100
56. Le Roch, K. G., Zhou, Y., Blair, P. L., Grainger, M., Moch, J. K., Haynes, J. D., De La Vega, P., Holder, A. A., Batalov, S., Carucci, D. J., and Winzeler, E. A. (2003) *Science* **301,** 1503–1508
57. Abrahamsen, M. S., Templeton, T. J., Enomoto, S., Abrahante, J. E., Zhu, G., Lancto, C. A., Deng, M., Liu, C., Widmer, G., Tzipori, S., Buck, G. A., Xu, P., Bankier, A. T., Dear, P. H., Konfortov, B. A., Spriggs, H. F., Iyer, L., Anantharaman, V., Aravind, L., and Kapur, V. (2004) *Science* **304,** 441–445
58. Aikawa, M., Hepler, P. K., Huff, C. G., and Sprinz, H. (1966) *J. Cell Biol.* **28,** 355–373
59. Przyborski, J. M., Wickert, H., Krohne, G., and Lanzer, M. (2003) *Mol. Biochem. Parasitol.* **132,** 17–26
60. Stanley, H. A., Langreth, S. G., and Reese, R. T. (1989) *Mol. Biochem. Parasitol.* **36,** 139–149
61. Hui, G. S., and Siddiqui, W. A. (1988) *Mol. Biochem. Parasitol.* **29,** 283–293
62. Wickert, H., Wissing, F., Andrews, K. T., Stich, A., Krohne, G., and Lanzer, M. (2003) *Eur. J. Cell Biol.* **82,** 271–284

Metabolism and Bioenergetics:

A *Plasmodium falciparum* Dipeptidyl Aminopeptidase I Participates in Vacuolar Hemoglobin Degradation

Michael Klemba, Ilya Gluzman and Daniel E. Goldberg

J. Biol. Chem. 2004, 279:43000-43007.
doi: 10.1074/jbc.M408123200 originally published online August 10, 2004